Gamma-ray remote sensing of soil properties in a forested area near Batlow, NSW.

P.N. Bierwirth[1], S.J. Aspin[1], P. J. Ryan[2], and N. J. McKenzie[3] .
[1]Australian Geological Survey Organisation
[2]CSIRO Forestry and Forest Products
[3]CSIRO Land and Water

Abstract
In forested and agricultural areas, reflective remote sensing methods are of limited utility for soil studies due to the variable effects of vegetation. Airborne gamma-ray remote sensing is presented here as a useful technique for soils. Short wavelength gamma-rays are detected from the upper 0.30-0.45 m of the soil . They are emitted from radioactive elements in the soil and largely pass through vegetation cover. In this paper, images of gamma parent elements (K, Th and U) are presented and element associations with soil properties and vegetation are analysed for a forested area near Batlow, NSW. Effects of vegetation are evident in gamma-ray data and in Landsat TM along powerlines and in clearings. A technique for removing this effect in the gamma-ray data is demonstrated. Detailed soil and rock chemistry together with ground gamma-spectrometer measurements were collected to support the interpretation and analysis of the image data. The work focuses mainly on the variation of soil properties within areas mapped as granodiorite lithology. Many areas of deep red soils are accurately mapped by the radiometric K data. The precise origin of these soils is not clear and their parent materials may include contributions from aeolian deposition, in situ weathering of granodiorite, and remnant basalt. . In areas of granodiorite, K patterns are interpreted to be a function of the degree of mineral weathering and can be related to soil depth and erosion status. This study demonstrates the effectiveness of gamma-ray remote sensing for directly mapping soil units and properties.

Introduction
A study was undertaken to investigate the spatial relationships of geology, soil and forest productivity in the Bago and Maragle State Forests near Batlow, NSW (Ryan et al., 1996). The study is part of a collaborative project between CSIRO Forestry and Forest Products, CSIRO Land and Water, State Forests of NSW, and AGSO The focus of this paper is on the use of airborne gamma spectrometric (AGS) data for the prediction of soil properties. Airborne geophysics, including gamma-spectrometry and magnetics was flown in February, 1996 across the complete survey area which is shown in Figure 1. This paper is concerned with a smaller study area wholely within the Bago State Forest (Figure 1).

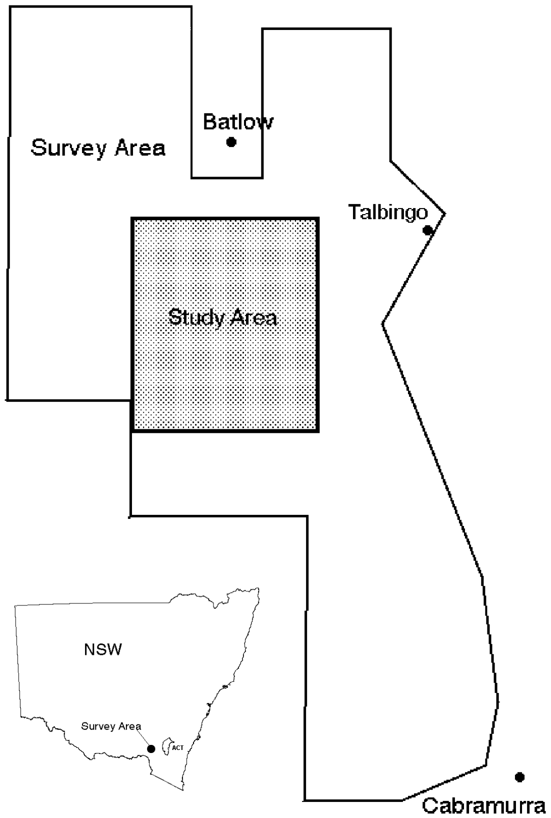

Figure 1. Location map of the study area within Bago State Forest. The outer border delineates the area covered by geophysical remote sensing.

AGS data uses raw gamma-ray wavelength data to derive abundances of the major gamma-emitting elements potassium (K), thorium (Th) and uranium (U). This provides spatial images of the geochemistry of the upper rock/soil layer. Gamma-rays are strongly attenuated and most of the radiation emanates from shallow ground depth - approximately 90% of measured gamma-rays are received from the top 0.3- 0.45 m for a dry overburden of density 1.5 Mg m^{-3} (Grasty, 1976). The abundances of the three elements are determined from spectrum windows but the 256 channel gamma spectrum is first smoothed by principal components (Hovgaard and Grasty, 1997). The airborne system collects a gamma-ray spectrum at points typically spaced about 70 m apart along profiles that, for this survey, are evenly spaced at 200 m apart. The derived K, Th and U abundances together with a total count are interpolated to create images that can be geographically rectified and converted to raster GIS coverages.

Gamma-element patterns generally relate to bedrock mineralogy and the weathering status of these minerals as influenced by the geomorphic stability and climate of a region (Wilford et al, 1997). Soil properties are a product of interacting environmental factors such as climate, parent material, topographry, organisms and time (Jenny, 1941 and 1980) with the whole process being called pedogenesis. Previous studies have shown that gamma element distributions can be related to important soil properties such as profile depth, texture, clay types, nutrient concentration, and acidity (Bierwirth et al., 1996; Bierwirth, 1997). In dissected terrain, relationships between AGS and soil properties depend strongly on lithology and degree of weathering (geomorphic stability). In flat terrain, AGS patterns may relate to parent materials (including alluvial sediment source) or pedogenic factors, such as degree of soil development, and becomes an important tool for mapping soil variations in the absence of geomorphic features (Bierwirth et al., 1996; Cook et al., 1996).

Vegetation effects on AGS data

The study area presents challenges for remote sensing and soil prediction due to the extensive cover of native and pine forest. Remote sensing techniques utilising surface reflectance such as Landsat TM, are usually ineffectual for mapping soils. Figure 2a shows a Landsat image for part of the area showing the vegetation cover and clearing along power lines. Figure 2b shows a potassium image for the same area. The powerline easements and the clearing to the west are visible indicating that vegetation does affect gamma-ray images. An earlier study of the same region used pine forest planting data and the Landsat data to determine the effects of vegetation on AGS element abundances (Aspin and Bierwirth, 1997). The loss of signal ranges from 13.5 to 21.9 percent (Table 1). It was concluded that gamma-ray data largely sees through even dense vegetation.

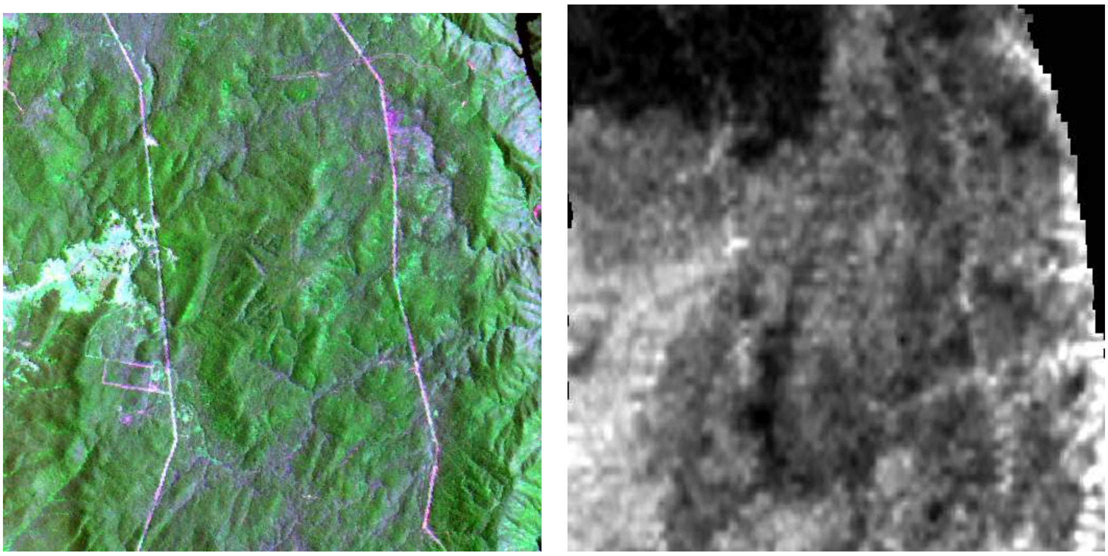

Figure 2. (a) Landsat image bands 1 4 7 = red, green and blue respectively, and (b) airborne potassium (K) as greyscale.

Table 1. Percent reduction of gamma-ray counts due to dense vegetation.

	K	Th	U
Pine Forest	20.0	14.0	13.5
Native Forest	21.9	14.1	16.4

Attenuation modelling to remove vegetation effects

This is a method developed for removing attenuation effects in multi-band imagery. The technique applied to gamma-ray data (Bierwirth, 1994) was adapted from work originally aimed at removing water depth effects from optical remote sensing imagery (Bierwirth et al., 1993). The idea was that an image could be derived where attenuation (ie. vegetation) effects were largely removed and variations in parent materials remained.

The absorption of gamma-ray photons by an attenuating medium is given by:

$$I_{ri} = I_{0i}\, e^{-u_i r} \qquad (1)$$

where I_{0i} is the intensity of gamma-rays emanating from a covered source in wavelength i and I_{ri} is the intensity after a distance r has been traversed through material with a linear absorption coefficient, u. By averaging over all wavelengths available, the depth of attenuating cover, r, can be represented by:

$$r = \sum_{i=1}^{N} \frac{\ln I_{ri}}{-u_i N} - \sum_{i=1}^{N} \frac{\ln I_{0i}}{-u_i N} \qquad (2)$$

where N is the number of wavelengths. The second term is set to a constant and a value of zero was used here. This is approximately equivalent to assuming that the average intensity of radiation sources is the same and that variation in the amplitude of the spectrum is due to attenuating cover. The derived attenuating thickness (r) can be calculated using band values (I_{ri}) and attenuation coefficients (u_i) derived for the appropriate density (Grasty, 1979). The value for overburden depth can then be substituted into equation 1 to derive the source intensity (I_{0i}) and effectively remove attenuation effects.

Results of this analysis for potassium data along the powerline easements are shown in Figure 3. Vegetation is effectively removed (see Figure 3b) from the original K data (Figure 3a). This is useful, particularly as an image enhancement technique for geological studies, but the process has also partly removed the effects of mineral weathering which is important for soil studies. The reason for this is that in some lithologies, eg granodiorite, loss of all radio-elements due to weathering will have a similar effect on the data as vegetation. Therefore the modified (K_0) image was not used for the following soils interpretation work.

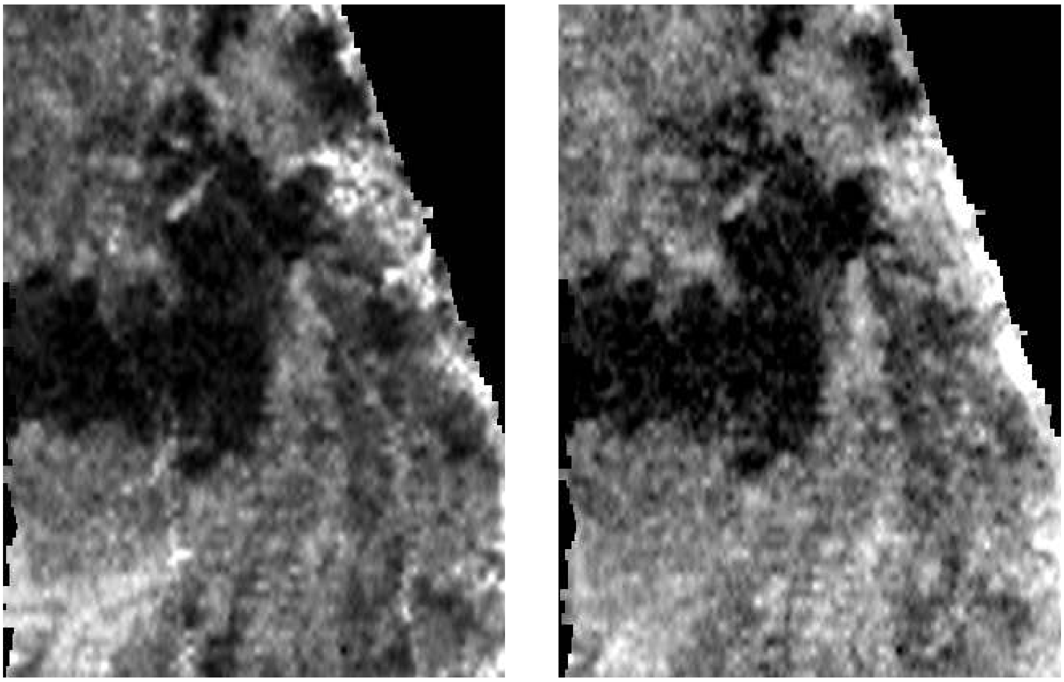

Figure 3. (a) Airborne measured potassium (K) concentration showing the effects of vegetation clearing along powerlines, and (b) K_0 derived from attenuation modelling with vegetation effects effectively removed.

Geology

Figure 4 shows a geology map for the study area for this paper (from Abell, 1998a). As noted earlier, the study area is a subset of the total survey area. The study area consists of Tertiary basalts (about 20 million years old) overlying Silurian granodiorite and some Ordovician gabbro. Sample sites for soil chemistry, X-Ray Diffraction (XRD) and X-Ray Fluorescence (XRF) analysis are shown. These sites were collected as part of a soil survey of the area that used as a design-based, two stage statistical sampling plan with geology, landform and climatic stratifying variables (Ryan et al., 1996).

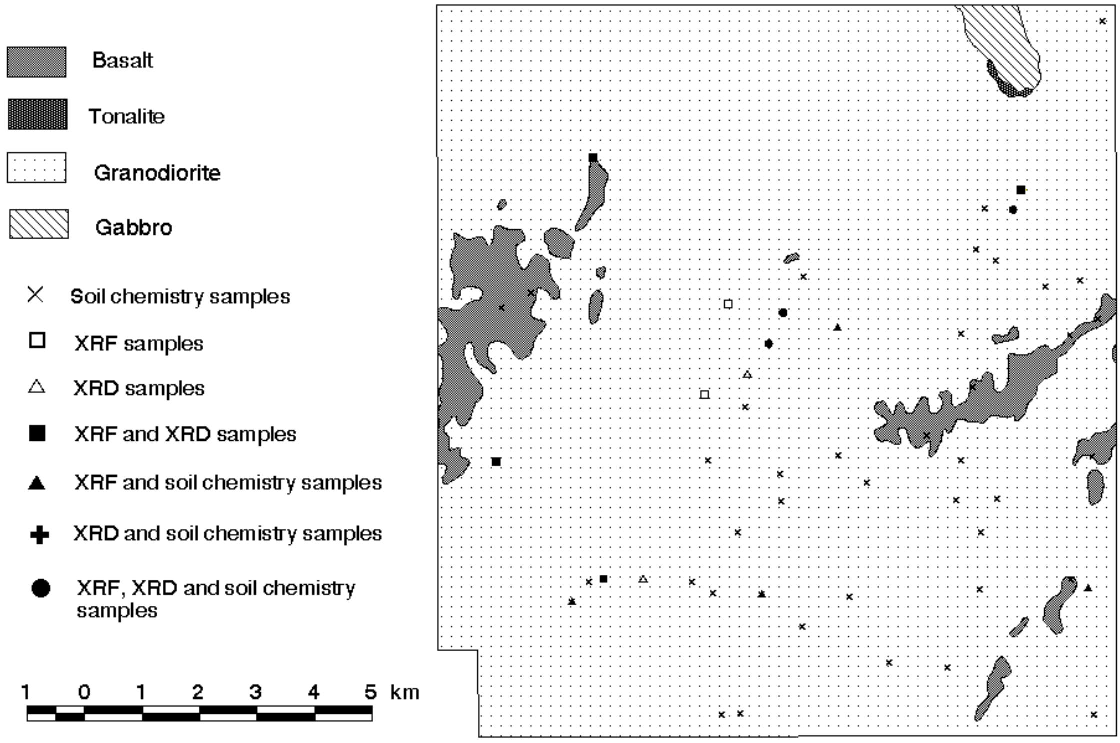

Figure 4. Geology and sample locations for the study area (from Abell, 1998a).

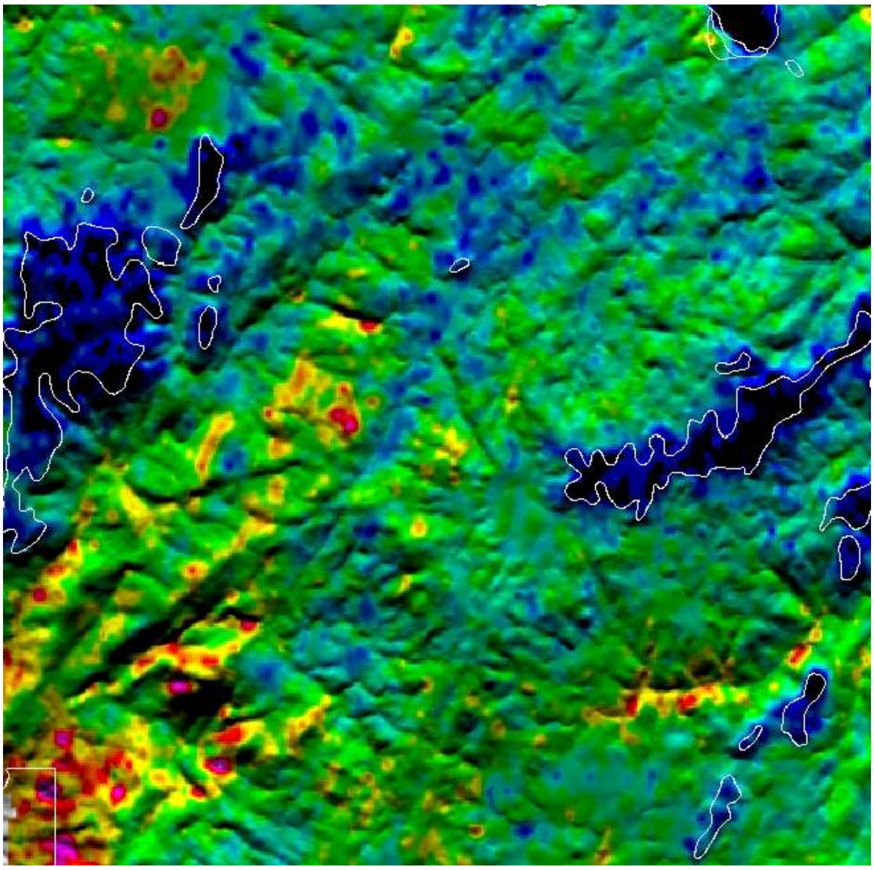

Figure 5. Potassium overlain on a 25 m hillshaded DEM. Red is high (2% K) through yellow, green, blue to black = low (0.3%)

Figure 5 shows the K image overlain on a 25 m DEM constructed from digital elevation contours, spot heights and streamlines (Ryan et al., 1996). Areas of basalt have a typically low K content. Granodiorite areas have a much higher K signature, with highest values corresponding to unweathered rock particularly evident where the plateaux is being incised and eroded. K, Th and U images are highly correlated in this area but the K data, being a more mobile element, shows generally greater variation due to rock-type and weathering. On the plateau there are low K areas (blue in Figure 5) that overlap with basalt in terms of gamma signature. From field inspection and soil-morphology descriptions these areas are identified as deep (> 2 m) red silty clay loam to silty clay soils (Red Dermosols and Red Kandosols (Isbell 1996) overlying granodiorite and other lithologies in the area. Evidence as to their origin is presented later.

Weathering and granodiorite soils

Field observations showed that variations of element patterns in the areas of granodiorite bedrock (particularly K) relate to weathering of parent materials and resulting soil morphology. High K areas (red to yellow in Figure 5) relate to erosionally active areas where less weathered materials, both bedrock and colluvium, are close to the surface. Conversely, low K areas (blue to green in Figure 5) cover a range of geomorphological aggraded, granodiorite soils, derived from both weathered saprolite and/or stable aggraded colluvium.. XRF data from a range of granodiorite rocks and overlying soils supports these observations (see Figure 6). Weathering indices such as the Miura weathering index (Selby, 1993) determines the ratio of more mobile elements to more residual ones. The Miura index is given by:

$$\frac{MnO + FeO + CaO + MgO + Na_2O + K_2O}{Fe_2O_3 + Al_2O_3}$$

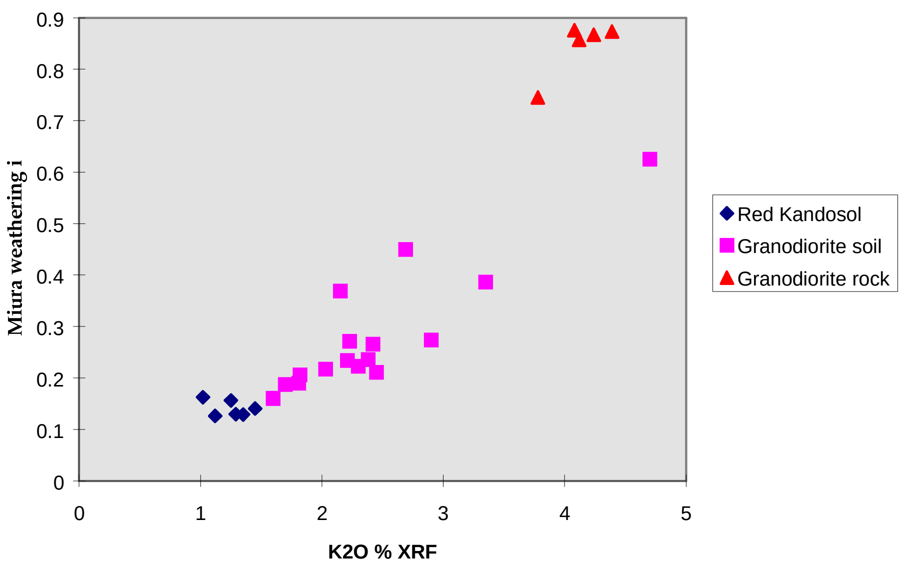

Figure 6. XRF results showing the relationship between K and the Miura weathering index for granodiorite rocks and the top 30 cm of overlying soils with granodiorite substrates

The soils termed 'granodiorite soils' in Figure 6 are soils overlying granodiorite, with observable granodiorite minerals and are not Red Kandosols. XRF potassium concentration in the samples generally relates to degree of weathering and this will also relate to airborne measured K. The soils with the lowest K concentration and Miura weathering index include a group of very deep, red clay soils. They are the most weathered but this is not necessarily evidence that they have formed completely from the underlying granodiorite.

AGS image relationships with soil properties

Soils analyses of samples collected from the surface 0.5 m were compared with nearest pixel image values for the radio-elements. Despite the limitations of comparing a radiometric footprint of about 100 m to a soil core, there are some useful correlations. Figure 7a and b show relationships between airborne K and soil sample total phosphorous and air-dry water content respectively. These relationships are largely controlled by lithological factors. Basalt has low K and high P concentrations and the derived soils have a larger air dry water content due to higher organic matter and clay contents. Soils formed on granodiorite have a lower K but higher air-dried water content than less weathered areas again because weathering increases clay content and hence soil moisture retention capacity.

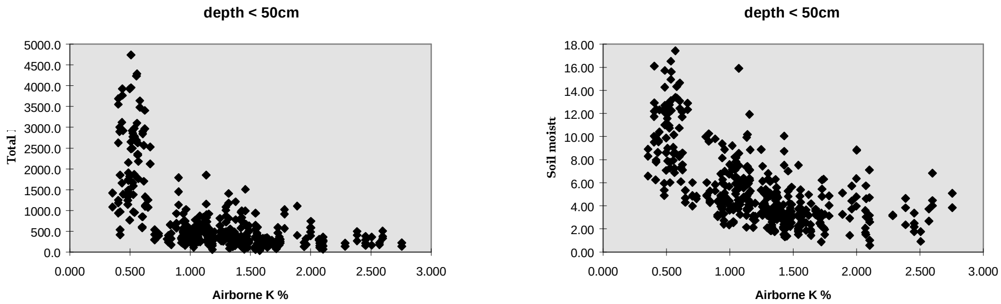

Figure 7. Relationships between airborne K and a) soil total phosphorous, and b) air-dried soil moisture samples from the top 0.5 m depth

Origin of the deep Red Kandosols

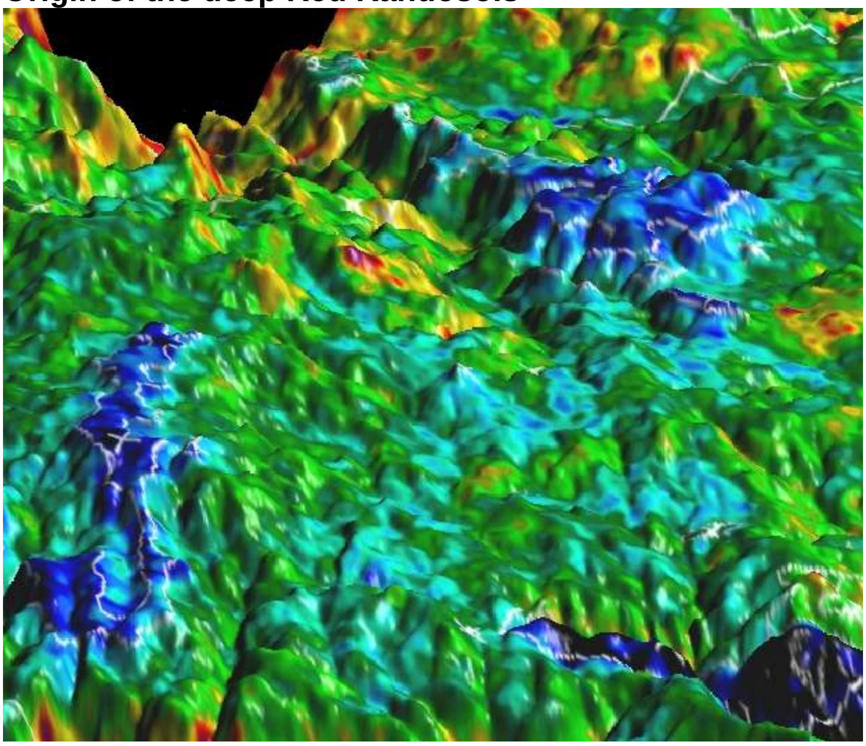

Figure 8. 3D perspective of study area, from the north-east corner, showing basalt flow in dark blue overlying the granodiorite. The deep red soils are associated with the light blue areas on the higher parts of the granodiorite plateau.

Figure 8 shows a 3D perspective, looking south-west, of the K image for the study area. The white lines are the geology boundaries from Figure 4. Basalt areas are clearly delineated as low K. In the granodiorite areas, light blue areas include the deep Red Kandosols overlying

weathered granodiorite. The origin of these deep red soils is still uncertain and their parent materials may include contributions from aeolian deposition, *in situ* weathering of granodiorite and remnant basalt. These areas could represent one the most stable remnants of an older plateau that has received aeolian dust input for most of the Holocene and Pleistocene. Evidence for a basalt influence includes the distribution patterns (see Figure 8) because the areas connect actual basalt outcrops.

XRF results for two resistant elements, phosphorous and titanium, for the red soils and lithology rocks and soils are presented in Figure 9.

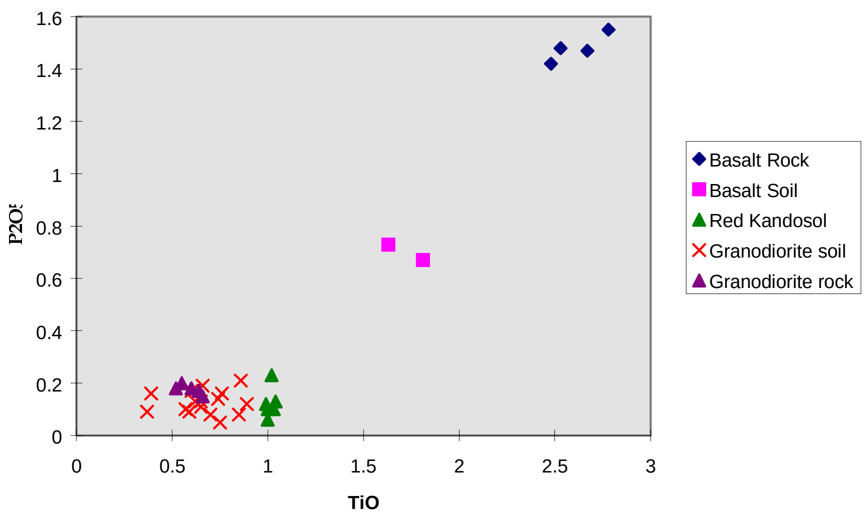

Figure 9. XRF analyses of TiO, P_2O_5 for Red Kandosols, granodiorite and basalt soils, and their parent materials.

Basalt rocks are high in both P and Ti. The levels in basalt derived soil are less but more than in granodiorite rocks and derived soils.. The Red Kandosols cannot not be distinguished from granodiorite soils or rocks in their P concentrations. For the more resistant Ti, there are higher concentration in the Red Kandosols although the granodiorite soils vary evenly from 0.4 to 1 %. One explanation is that the Red Kandosols have a basalt origin but have been severely weathered to remove both the P and Ti.. An alternative theory is that aeolian material, which has a low P (equivalent to that of granodiorite) and Ti concentration higher than granodiorite, has diluted the basalt soil and modified the older granodiorite soils. The other possibility is that the deep Red Kandosols have formed *in situ* on granodiorite, although this doesn't explain higher Ti values.

Radioelement soil association map

Figure 10 shows a soil class map derived solely from the remotely sensed potassium data. Boundaries from geological mapping (Abell, 1998a) have been used to separate basalt areas, gabbro areas and alluvial swamps from remaining areas. Further subdivision within the granodiorite was based on field observations and regolith landform mapping of the area (Abell, 1998b). This has produced three classes defined on K values for the area mapped as granodiorite geology: 1) shallow soils associated with unweathered granodiorite materials, 2) deeper soils and weathered granodiorite saprolite and 3) deep Red Kandosols. Some of the areas around the basalts, that are classed as Red Kandosols, are undoubtedly missclassified and related to basalt colluvium.

Other work has demonstrated that thorium complexes with iron-oxides during weathering and the Th image data can map gradations between fresh bedrock and deep weathered soils (Street, 1998; Dickson and Scott, 1997). XRF data for four samples from this area also

demonstrated this but it was decided that this was insufficient evidence to subdivide the basalt and gabbro areas based on Th data.

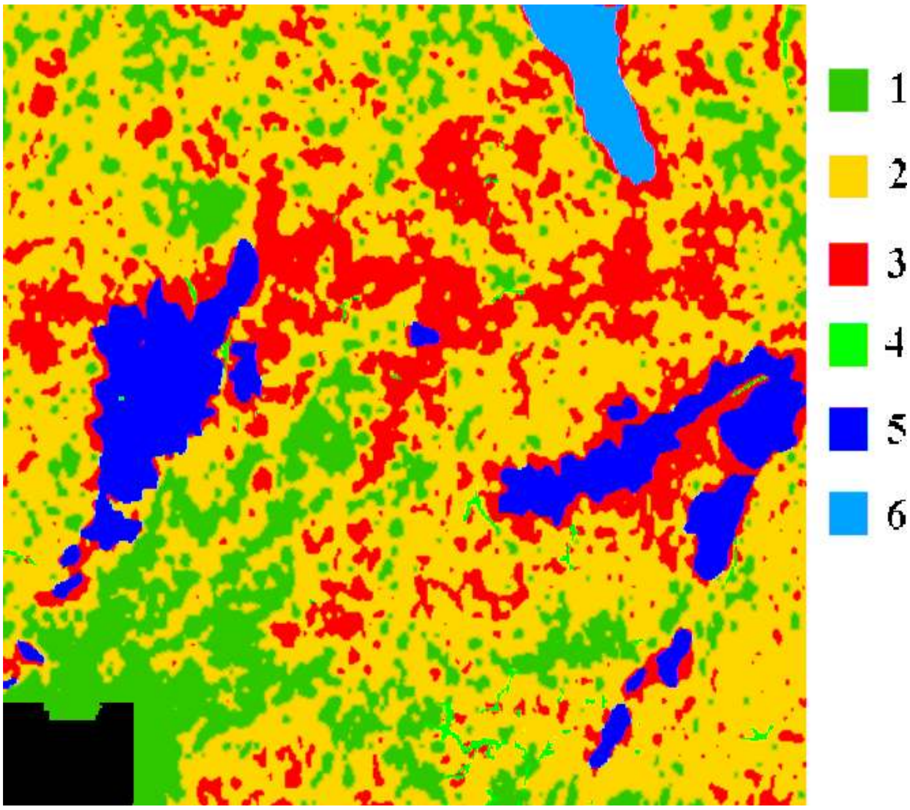

Figure 10. Soil class map using K and mapped geological boundaries. Classes are labelled as follows:

1) Granodiorite bedrock and colluvium - shallow soils, relatively unweathered, erosionally active areas (K > 1.5%)
2) Granodiorite saprolite and weathered colluvium - deeper soils, erosionally inactive (K = 1 - 1.5%)
3) Red Kandosols - deep (> 2 m) red silty clay loam to silty clay soils (K < 1%)
4) Alluvial swamps
5) Soils on Basalt
6) Soils on Gabbro

It should be pointed out that the relationships above between radiometric K and soil classes hold for this particular sub-area. In other areas, low K may relate to leached or sandy materials in depositional sites. In other words, geomorphic and geologic stratification should be attempted before modelling gamma-ray data. This type of modelling relates mainly to mineral weathering and does not account for climatic and terrain influence on soil forming processes. A numerical soil classification procedure has been developed for the larger Bago-Maragle study area that incorporates terrain and climatic variables to predict soils (Ryan and McKenzie *pers. comm.*). In this classification, the gamma-ray data are key predictors.

Conclusions

This study has shown that gamma-radiometric data are very useful for predicting the character and distribution of soil properties, particularly in forested or vegetated landscapes. Dense pine and eucalypt forest attenuates only 15-20% of gamma-radiation . Modelling of this attenuation effect allowed the removal of the vegetation.

In the Bago-Maragle study area soils with high nutrient levels formed from basalt together with deep Red Kandosols can be distinguished by low airborne potassium (0.3 to 1%K) from granodiorite soils. The degree of weathering in soils formed from granodiorite can also be mapped using the airborne K image data.

AGS data have the potential to greatly improve the accuracy and efficiency of soil mapping

Acknowledgements

The authors wish to acknowledge the work of Julie Kamprad of AGSO for the XRD interpretation. John Pyke and Bill Pappas produced the XRF results for this work. We also thank Peter Leppert and David Jacquier for soil chemical anayses and soil sampling respectively.

References

Abell, R. S., 1998a. Bedrock geology of the Greenhills-Bago-Maragle state forest, NSW. (1:100,000 scale map) AGSO, Canberra.

Abell, R. S., 1998b. Regolith Landforms of the Greenhills-Bago-Maragle state forest, NSW. (1:100,000 scale map) AGSO, Canberra.

Aspin, S. J. and P. N. Bierwirth, 1997. GIS analysis of the effects of forest biomass on gamma-radiometric images. *Proceedings 3rd National Forum on GIS in the Geosciences,* AGSO record 1997/36, p77-83.

Bierwirth, P.N., T. J. Lee, R. V. Burne, 1993. Shallow sea-floor reflectance and water depth derived by unmixing multispectral imagery. *Photogrammetric Engineering and remote Sensing,* 59, (3), pp331-338.

Bierwirth, P. N., 1994. Image Processing of Airborne Gamma-Ray Data for Soils Information - Wagga Wagga, NSW, *7th Australasian Remote Sensing Conference Proceedings*, Melbourne. P927 - 934.

Bierwirth, P. N., P. E. Gessler, and D. McKane, 1996. Empirical investigation of airborne gamma-ray images as an indicator of soil properties - Wagga Wagga, NSW. In *8th Australasian Remote Sensing Conference Proceedings*. Canberra. Thursday, p81-89.

Bierwirth, P. N., 1997. The use of airborne gamma-emission data for detecting soil properties. *Proceedings of the Third International Airborne Remote Sensing Conference and Exhibition*, Copenhagen, Denmark.

Cook, S. E., R. J. Corner, R. J. Groves and Grealish, G, 1996. Application of airborne gamma radiometric data for soil mapping. Australian Journal of Soil Research. 34, p183-194.

Dickson, B.L., and K. M. Scott, 1997. Interpretation of aerial gamma-ray surveys - adding the geochemical factors. *AGSO Journal of Australian Geology and Geophysics*, 17 (2) p187 - 200.

Gessler, P. E., 1996. *Statistical soil-landscape modelling of environmental management.* PhD Thesis, Australian National University,.

Grasty. R. L., 1997. Radon emanation and soil moisture effects on airborne gamma-ray measurements. *Geophysics,* 62 (5) p1379 - 1385.

Grasty, R.L. 1976. Applications of gamma radiation in remote sensing. In *Remote Sensing for Environmental Sciences*, ed. E. Schanda, Springer Verlag, Berlin. p. 257,.

Grasty, R.L. 1994. Summer outdoor radon variations in Canada and their relation to soil moisture. *Health Physics*, Vol. 66, No. 2, pp. 185-193.

Hovgaard, J., and R. L. Grasty, 1997. Reducing statistical noise in airborne gamma-ray data through spectral component analysis. In *Proceedings of Exploration 97: Fourth Decennial Conference on Mineral Exploration* edited by A.G. Gubins, 1997, 753-764.

Isbell, R.F., 1996. *The Australian Soil Classification*. CSIRO Publishing: Melbourne.

Jenny, H., 1941. *Factors of Soil Formation - A System of Quantitative Pedology.* McGraw-Hill: New York.

Jenny, H., 1980. *The Soil Resource - Origin and Behaviour.* Springer-Verlaag: New York.

Ryan, P.J, N. J. McKenzie, A. Loughhead, L. Ashton, 1996. New methods for forest soil surveys. In: *Environmental Management: The Role of Eucalypts and other Fast Growing Species*. Editors K.G. Eldridge, M.P. Crowe and K.M. Old Eds. CSIRO Publishing, Collingwood.

Selby, M. J., 1993. *Hillslope materials and processes*. Oxford University Press

Street, M. K., R. M. Johnston, and P. N. Bierwirth, 1998. Airborne Gamma-ray spectrometry, a tool for land management - The Liverpool Plains NSW. *AGSO Record* (in prep)

Wilford, J.R., P. N. Bierwirth, and M. A. Craig, 1997. Application of airborne gamma-ray spectrometry in soil/regolith mapping and applied geomorphology. *AGSO Journal*, vol 17, no 12, p201-216.